Composite Structures 277 (2021) 114618

Contents lists available at ScienceDirect

Composite Structures

journal homepage: www.elsevier.com/locate/compstruct

Numerical parametric investigation on the moment redistribution of basalt FRC continuous beams with basalt FRP bars

Abdelrahman Abushanab [a], Wael Alnahhal [b,*]

[a] Department of Civil and Architectural Engineering, Qatar University, Doha, Qatar
[b] Department of Civil and Architectural Engineering, College of Engineering, Qatar University, Doha, Qatar

ARTICLE INFO

Keywords:
Parametric study
Moment redistribution
BFRP bars
Basalt fibers
Continuous beams

ABSTRACT

Recently, researchers' efforts have been directed toward using fiber-reinforced concrete (FRC) in lieu of conventional concrete to improve the compressive strain, tensile strength capacity, cracking patterns, and ductility of fiber-reinforced polymer (FRP) reinforced concrete members. In this study, a numerical one-factor-at-a-time parametric study including 144 finite element (FE) models was performed using ABAQUS 6.14 software to deeply explore the influence of the volume ratios of basalt macro-fiber (BMF), reinforcement ratios of basalt FRP (BFRP) bars, and stirrups spacing on the moment redistribution of basalt FRC continuous beams reinforced with BFRP bars. It was shown that the most influential parameter on the moment redistribution was the longitudinal reinforcement configuration. While a higher moment redistribution was noticed with higher sagging reinforcement ratios and BMF, stirrups spacing showed no effect on the moment redistribution. It was also observed that the moments were inversely distributed for FE models having high hogging-to-sagging reinforcement ratios. The sagging-to-hogging reinforcement ratio is recommended to be at least 1.6 to ensure a uniform moment redistribution. Furthermore, a multiple linear regression model was developed using Minitab 17 software to establish a relationship between the investigated parameters and the beams' moment redistribution. The moment redistribution was accurately predicted using the developed regression model.

1. Introduction

Corrosion of steel reinforcement degrades the strength and durability properties of reinforced concrete (RC) structures while increasing maintenance costs [1]. To address this issue, various innovative solutions have been proposed, one of which is the use of non-corrosive fiber-reinforced polymer (FRP) composites. Compared to steel reinforcement, FRP composites have a higher strength-to-weight ratio and excellent durability properties [2]. Glass FRP (GFRP), aramid FRP (AFRP), and carbon FRP (CFRP) are the most commonly used FRP composites [3–5]. With the advancement of FRP composite production technology, newly developed basalt FRP (BFRP) composites were eventually added to the FRP family [6]. BFRP composites have 25% lesser weight than steel, higher resistance to chemical attacks and lower impact on the environment than GFRP, and larger ultimate strains and lower price than CFRP [7–9].

Numerous studies have been reported on the behavior of simply-supported RC elements with FRP reinforcement [8,10–16]. However, little attention has been given to the behavior of continuous beams and slabs reinforced with FRP bars [17–21]. Habeeb and Ashour [3], Grace et al. [22], and Ashour and Habeeb [23] observed that the cracking patterns, failure mode, and ductility of FRP-RC continuous beams were different from those with steel reinforcement. Mahroug et al. [24] and Akiel et al. [25] noticed that the sagging reinforcement was more effective in improving the stiffness of CFRP-RC continuous slabs than the hogging reinforcement. Furthermore, current design codes allow continuous steel-RC beams and slabs to redistribute bending moments between critical sections during loading [26,27]. This distinctive property allows to reduce the congested reinforcement at critical connections and for a maximum utilization of the members' loading capacity [28,29]. The moment redistribution in steel-RC members has been extensively investigated [30–33]. However, there is little data on FRP-RC continuous beams and slabs [3,18,29,34–36]. Mahroug et al. [24] demonstrated that the redistribution of bending moments in FRP-RC elements depends on the reinforcement configuration, lower elastic modulus of FRP composites compared to steel reinforcement, and bond strength of FRP bars to concrete. Mahrouget al. [20] and Kara et al. [37] reported that BFRP-RC slabs with higher sagging reinforcement

* Corresponding author.
E-mail addresses: aa1104287@qu.edu.qa (A. Abushanab), wael.alnahhal@qu.edu.qa (W. Alnahhal).

https://doi.org/10.1016/j.compstruct.2021.114618
Received 25 June 2021; Accepted 30 August 2021
Available online 4 September 2021

recorded higher moment redistribution. Additionally, EI-Mogy et al. [38] observed higher moment redistribution in GFRP-RC continuous beams having higher stirrup diameters. A recent study by Akiel et al. [19] showed that RC continuous beams with only BFRP bars reported higher moment redistribution than those with hybrid reinforcement of BFRP and steel bars. Moreover, the authors reported that increasing the top reinforcement inversely affected the moment redistribution. It is worth mentioning that due to the brittleness of FRP composites, the moment redistribution of FRP-RC continuous members was exempted from FRP design guidelines [39–42]. Accordingly, additional research on the moment redistribution of FRP-RC continuous elements is required to provide more confidence in FRP design procedures.

Meanwhile, FRP-RC elements suffer from the low elastic modulus and linear elastic stress–strain response to failure, which cause excessive deformations, wider cracks, and brittle failure compared to their counterparts with steel reinforcement [8,14]. As a result, ACI 440.1R-15 [39] recommends that FRP-RC elements should be over-reinforced to avoid FRP bar rupture and to ensure concrete crushing failure mode. Consequently, the tensile strength of FRP reinforcement in FRP-RC elements is not fully exploited, as the failure is mainly determined by concrete properties. Therefore, researchers have focused their efforts on the use of fiber-reinforced concrete (FRC) to improve the compressive strain of concrete and the ductility of FRP-RC elements [10,43–45]. Wang and Belarbi [43] studied the influence of adding polypropylene fibers on the flexural behavior of CFRP and GFRP-RC beams. The authors found that FRC specimens had higher tensile strength and lower crack widths. Similar outcomes were also reported by High et al. [10] and Yang et al. [44]. A study conducted by Issa et al. [45] showed that steel, glass, and polypropylene fibers increased the ductility of GFRP-RC beams by 277.8% in comparison with plain GFRP-RC beams. Furthermore, the beams' load-carrying capacity was increased by increasing the fibers' volume fractions (V_f). Moreover, Visintin et al. [46] and Abushanab et al. [47] found that structural fibers enhanced the moment redistribution of continuous beams by 17%.

Steel and synthetic fibers are currently the most often used fibers in FRC applications. Nonetheless, the inclusion of steel fibers in FRC increases the FRC weight and susceptibility to corrosion. Besides, synthetic fibers show a sign of degradation against environmental and chemical attacks [14]. For that reason, the feasibility of replacing steel and synthetic fibers with the recently developed basalt macro-fibers (BMF) was investigated in this study. Limited studies are available on the performance of basalt fibers on FRP-RC beams and slabs [2,6,14,48,49]. Attia et al. [14] revealed that BMF improved the load-crack responses of BFRP-basalt FRC (BFRC) slabs by 46% to 93% and resulted in a more ductile failure mode. Similar observations were also reported by Abed and Alhafiz [2].

In previous research done by the authors, the moment redistribution of BFRC continuous beams with BFRP bars was investigated experimentally and analytically [47,50]. Seven BFRP-BFRC continuous beams with various V_f of BMF, longitudinal reinforcement ratios, and stirrups spacing, were investigated. The experimental results showed that increasing the main reinforcement and BMF ratios increased the moment redistribution by 43% and 17%, respectively. However, stirrups spacing showed negligible influence on the beams' moment redistribution. Furthermore, the authors developed and validated 2D nonlinear finite element (FE) models using ABAQUS software [51]. The beams' load–deflection responses and cracking patterns were accurately predicted by the developed FE models. However, because of the small number of the tested continuous large-scale beams due to equipment and experiment restrictions, a thorough examination of all parameters impacting the moment redistribution of BFRC continuous beams with BFRP bars was challenging. Therefore, the present study aimed to perform a numerical one-factor-at-a-time parametric study to explore additional parameters influencing the moment redistribution of BFRC continuous beams with BFRP bars. Moreover, a multiple linear regression model was established to describe the relationship between the beams' moment redistribution and reinforcement ratios, V_f of BMF, and stirrups spacing. It is expected that this study would contribute to the FRP design guidelines.

2. Summary of the experimental and numerical work

The current study builds on the authors' earlier research on the moment redistribution of BFRP-BFRC continuous beams [47,50]. A total of seven BFRP-BFRC continuous beams made of two-equal span were experimentally tested and numerically simulated. The beams' cross-section dimension was 200 × 300 mm. The beams' overall length was 4000 mm with an effective span length of 1800 mm. A schematic drawing of the beam specimen is shown in Fig. 1. The beams were longitudinally reinforced with helical wrapping surface BFRP bars of 8 and 10 mm diameters with an ultimate tensile strength of 1096 and 1070 MPa, ultimate strain of 0.027 and 0.023, and elastic modulus of 42.7 and 44.7 GPa, respectively. In addition, steel stirrups with a diameter of 10 mm, yield tensile strength of 515 MPa, and yield strain of 0.00268 were used as transverse reinforcement for all beams. BMF of 46% vinyl ester, 43 mm length, 0.66 mm diameter, 1100 MPa ultimate tensile strength, 0.021 ultimate strain, and 44 GPa elastic modulus were added to BFRC beam specimens. Fig. 2 shows photographs of BFRP bars and BMF used in the previous study. Moreover, the tested beams were numerically simulated using commercial ABAQUS software [51]. The developed FE model is presented in Fig. 3. BFRC compressive stress–-strain behavior was modeled based on Ayub et al. analytical model [52], while the tensile behavior of BFRC was modeled identical to the experimental data. The effect of the BMF in the FE models was implicitly included in the compressive and tensile strengths of BFRC. The built-in concrete damage plasticity (CDP) model was used to simulate the compressive and tensile damage of concrete. BFRP bars and steel stirrups were models as truss elements. Material non-linearity and mesh sensitivity were considered in the developed FE models. The FE models were validated using the load–deflection and cracking responses of the tested beams. Further details on the experimental and numerical programs can be found in [47,50].

3. The parametric study

The developed FE model in Abushanab [50] was systematically expanded to 144 FE models to study all possible combinations of reinforcement ratios, V_f of BMF, and stirrups spacing on the moment redistribution of BFRP-BFRC continuous beams, as shown in Table 1. The investigated parameters included four top and bottom BFRP longitudinal reinforcement ratios ($0.6\rho_{fb}$, $1.0\rho_{fb}$, $1.8\,\rho_{fb}$, and $2.8\,\rho_{fb}$, where ρ_{fb} is FRP balanced reinforcement ratio), three V_f of BMF (0, 0.75, and 1.5%), and three stirrup spacings (80, 100, and 120 mm). All FE models had identical geometry and loading patterns to the tested beams. A one-factor-at-a-time parametric study was carried out on the developed FE models. To investigate the impact of a given parameter, only this parameter was varied while the other parameters were kept unchanged. For a given FE model, the moment redistribution was calculated as per Eqs. (1) to (5):

$$M_{S-Pred.} = R_A \times \left(\frac{L}{2}\right) \tag{1}$$

$$M_{H-Pred.} = \left(\frac{P}{2} \times \left(\frac{L}{2}\right)\right) - R_A \times L \tag{2}$$

$$M_{S-Elastic} = 0.156 \times \frac{P}{2} \times L \tag{3}$$

$$M_{H-Elastic} = 0.188 \times \frac{P}{2} \times L \tag{4}$$

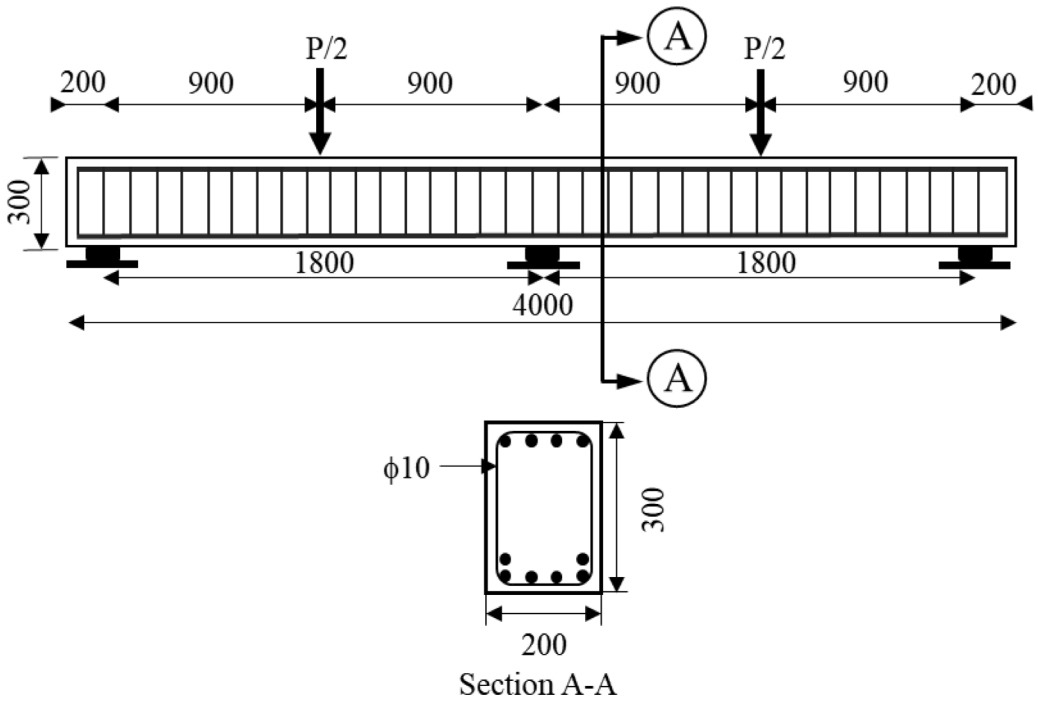

Fig. 1. Schematic drawing of the beam specimens. All dimensions are in mm.

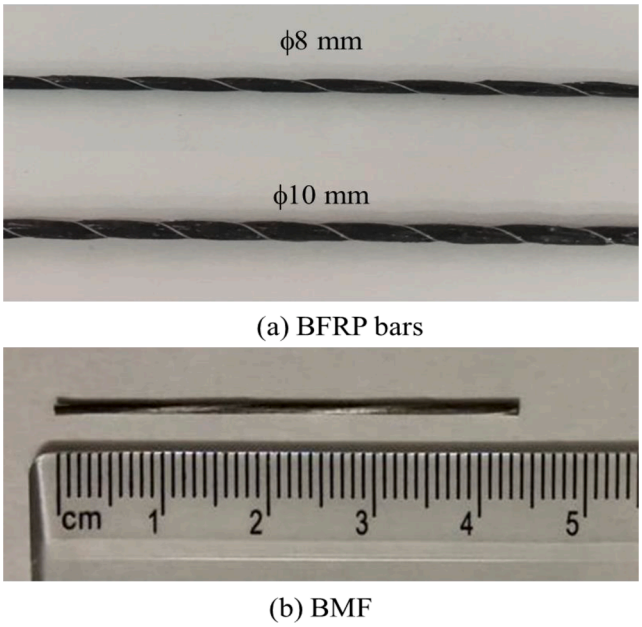

Fig. 2. BFRP bars and BMF used in Abushanab et al. [47].

$$\%\text{Moment Redistribution} = \frac{M_{\text{Pred.}} - M_{\text{Elastic}}}{M_{\text{Elastic}}} \times 100 \quad (5)$$

where $M_{S\text{-Pred.}}$ is the predicted sagging moment by the FE model, $M_{H\text{-Pred.}}$ is the predicted hogging moment by the FE model, $M_{S\text{-Elastic}}$ is the elastic sagging moment, $M_{H\text{-Elastic}}$ is the elastic hogging moment, R_A is the end reaction measured by the FE model, and P is the total applied load measured by the FE model. Afterward, a multiple linear regression equation relating the predicted moment redistribution to the investigated parameters was proposed using Minitab 17 software [53]. The equation was then verified against the experimental moment redistribution.

3.1. Analysis of the results

3.1.1. Effect of BFRP reinforcement ratio

The reinforcement ratios considered in this parametric study are classified as under-reinforcement, balance-reinforcement, and over-reinforcement ratios, as shown in Table 1. The details of the reinforcement ratios used in this parametric study are shown in Table 2, and the testing matrix of the FE models is presented in Table 3. The designation used for the FE models is based on the reinforcement configuration. The first part stands for the hogging reinforcement, while the second part stands for the sagging reinforcement. R0, R1, R2, and R3 stand for the reinforcement ratios of $0.6\rho_{fb}$, $1.0\rho_{fb}$, $1.8\ \rho_{fb}$, and $2.8\ \rho_{fb}$, respectively. For example, R0R1 represents a FE model with a hogging reinforcement of 2 ϕ 8 and sagging reinforcement of 2 ϕ 10. The testing matrix, shown in Table 3, was repeated for each level of the BMF and stirrups spacing, making a total of 144 FE models.

The predicted moment redistributions of BFRP-BFRC continuous beams with different hogging and sagging reinforcement ratios are presented in Fig. 4(a)–(d). It could be seen that at constant hogging reinforcement ratios of R0 and R1, the moment redistribution increased as the sagging reinforcement ratio increased from R0 to R3. At V_f of BMF of 0% and stirrups spacing of 120 mm, FE models R0R1, R0R2, R0R3, R1R1, R1R2, and R1R3 reported 20%, 90%, 120%, 100%, 200%, and 280% higher moment redistribution than their counterparts with a hogging reinforcement ratio of R0, respectively. This is attributed to the increased flexural rigidity of the sagging section with higher sagging reinforcement ratios, which, in turn, allowed the sagging section to resist more tensile stresses. A similar trend was also observed for FE models with BMF at $V_f = 0.75$ and 1.5% and stirrups spacing of 80 and 100 mm. El-Mogy et al. [29] and Santos et al. [54] have also confirmed that the moment redistribution of FRP-RC continuous beams increased by increasing the sagging reinforcement ratio.

Conversely, it was observed that increasing the hogging reinforcement ratio to R2 and R3 while keeping the sagging reinforcement at R0 and R1 resulted in an inverse moment redistribution (i.e., from sagging to hogging section), which is similar to the experimental observation reported by the authors in an earlier study [47]. The inverse moment redistribution occurred because the sagging reinforcement in FE models

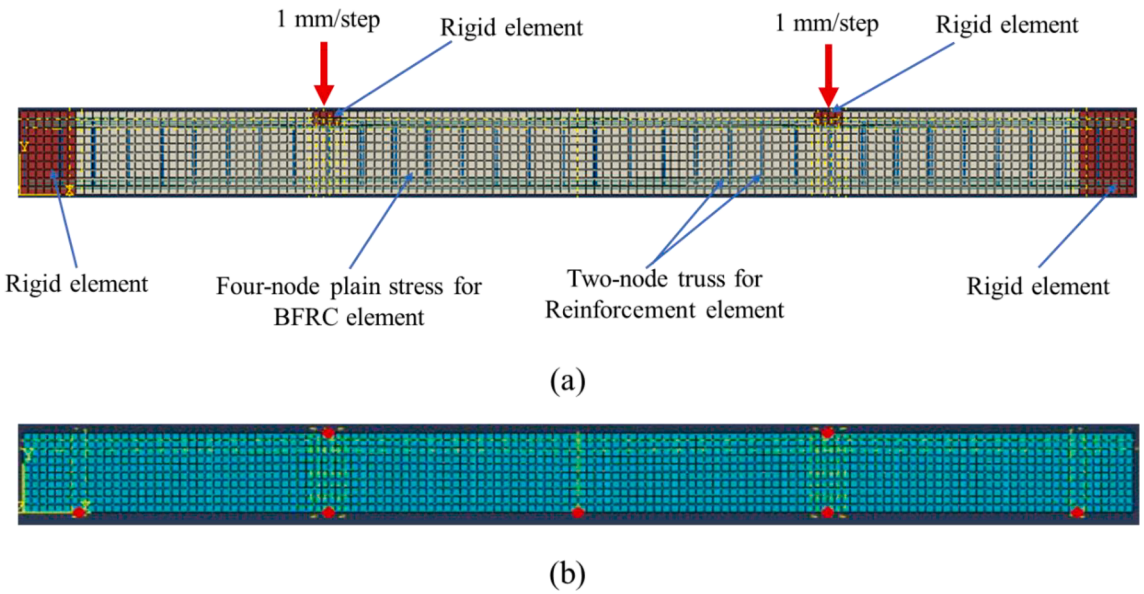

Fig. 3. The developed FE model in Abushanab [50]: (a) loading patterns and element types and (b) node locations.

Table 1
Studied parameters and their levels.

Parameter	Unit	Level 1	Level 2	Level 3	Level 4
Top reinforcement ratio	ρ_{fb}	0.6	1.0	1.8	2.8
Bottom reinforcement ratio	ρ_{fb}	0.6	1.0	1.8	2.8
V_f of BMF	%	0	0.75	1.5	–
Stirrup spacings	mm	80	100	120	–

Note:
1- ρ_{fb} is the FRP balanced reinforcement ratio. ρ_{fb} was calculated as per ACI 440.1R-15 provisions [39].

Table 2
Reinforcement configuration of the simulated beams.

Symbol	Reinforcement	ρ_f	ρ_f/ρ_{fb}
R0	2 ϕ 8	0.00167	0.64
R1	2 ϕ 10	0.00262	1.00
R2	4 ϕ 10	0.00523	2.00
R3	6 ϕ 10	0.00760	3.00

Table 3
Testing matrix of the simulated beams.

Hogging Reinforcement	Sagging Reinforcement			
	R0	R1	R2	R3
R0	R0R0	R0R1	R0R2	R0R3
R1	R1R0	R1R1	R1R2	R1R3
R2	R2R0	R2R1	R2R2	R2R3
R3	R3R0	R3R1	R3R2	R3R3

R2R0, R3R0, and R3R1 could not provide the flexural strength needed to sustain the applied stresses and thus transferred part of the sagging stresses to the hogging section. This observation agrees with Akiel et al. [19] and El-Mogy et al. [29]. On the other hand, FE models R2R1, R2R2, and R3R2 showed a uniform moment redistribution (i.e., from hogging to sagging section) of only 2%, 8%, and 7%, respectively. This is mostly due to the increased axial stiffness of BFRP bars at the hogging section, which decreased the middle support crack widths and allowed them to withstand higher tensile stresses. As a result, these models transferred less tensile stresses to the sagging section in comparison with other FE models with higher sagging-to-hogging ratios (i.e., FE models R2R3 and R3R3). In light of these results, it is clear that the higher the sagging-to-hogging reinforcement ratio, the better the moment redistribution, and vice versa. This implies that the reinforcement configuration of BFRP-BFRC continuous beams had a significant influence on the moment redistribution. Based on the findings, BFRP-BFRC continuous beams should be designed with a sagging-to-hogging reinforcement ratio of at least 1.6 to ensure a uniform and effective moment redistribution.

3.1.2. *Effect of BMF*

The effect of BMF on the moment redistribution of BFRP-BFRC continuous beams was investigated on 144 FE models with V_f of 0, 0.75, and 1.50% (Fig. 4(a)–(d)). It is clear that FE models with BMF achieved higher moment redistribution than those with no added BMF. This could be demonstrated in FE model R1R3 with stirrups spacing of 80 mm, where increasing the V_f of BMF from 0% to 0.75% and 1.5% increased the moment redistribution by 13% and 19%, respectively, attributable to the fibers' bridging effect, which redistributed the tensile stresses along the whole length of the beams and therefore increased their rotational capacity. The results also demonstrated that when the sagging reinforcement increased, the influence of BMF on the moment redistribution decreased. For example, FE models R0R1, R0R2, and R0R3 with BMF at $V_f = 1.5\%$ and stirrups spacing of 100 mm recorded 18, 12, and 9% higher moment redistribution than their counterparts with no BMF, respectively. This behavior could be explained by the relationship between the beams' sagging reinforcement and tensile cracks, of which increasing the sagging reinforcement decreased the tensile cracks, and thus decreasing the effect of BMF compared to the beams with lower sagging reinforcement ratios. The results of Abed and Alhafiz [2], Attia et al. [14], and Alnahhal and Aljidda [55] and also reported that BMF improved the ductility and rotational capacity of RC elements.

3.1.3. *Effect of stirrups spacing*

The variations in the beams' moment redistribution with respect to the stirrups spacing are provided in Fig. 4(a)–(d). Each level of stirrups spacing is composed of 48 FE models. According to the earlier experimental study conducted by the authors [47], it was observed that the moment redistribution was marginally increased by 6% when the stirrups spacing decreased from 120 to 80 mm. It should be emphasized that this discovery was reported based on a single beam experiment. However, a deeper investigation into the effect of stirrups spacing on moment redistribution in this parametric study revealed that there is no clear

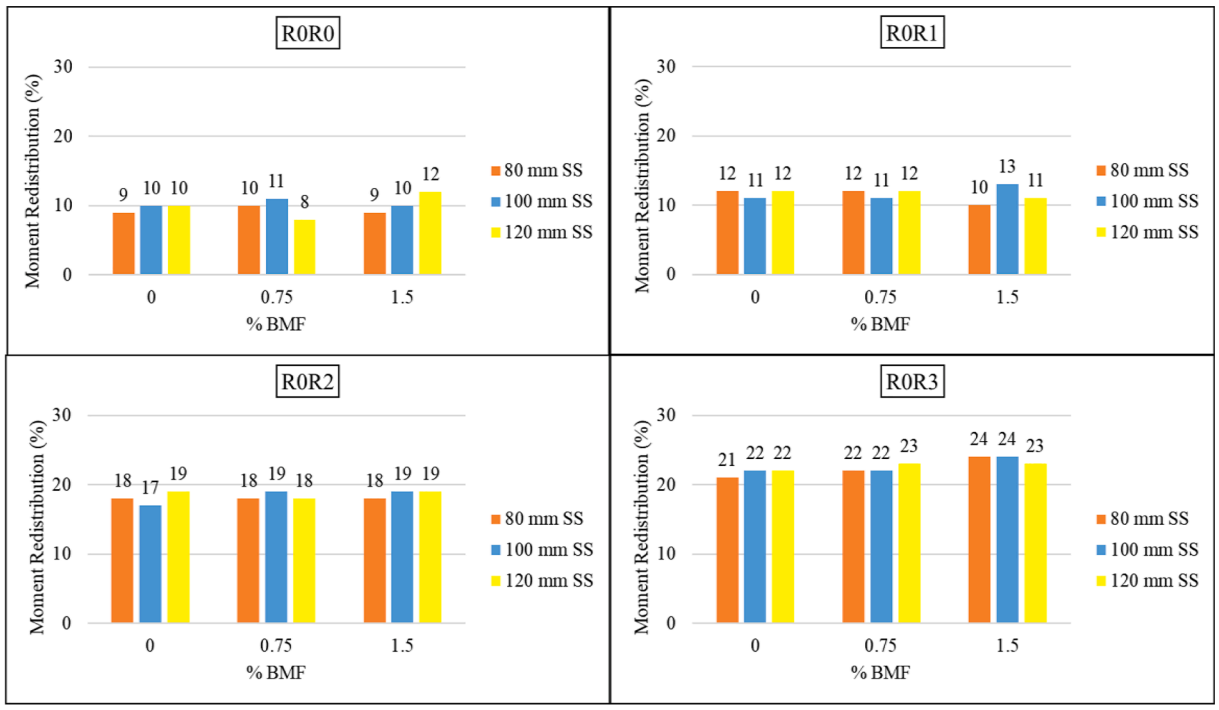

(a)

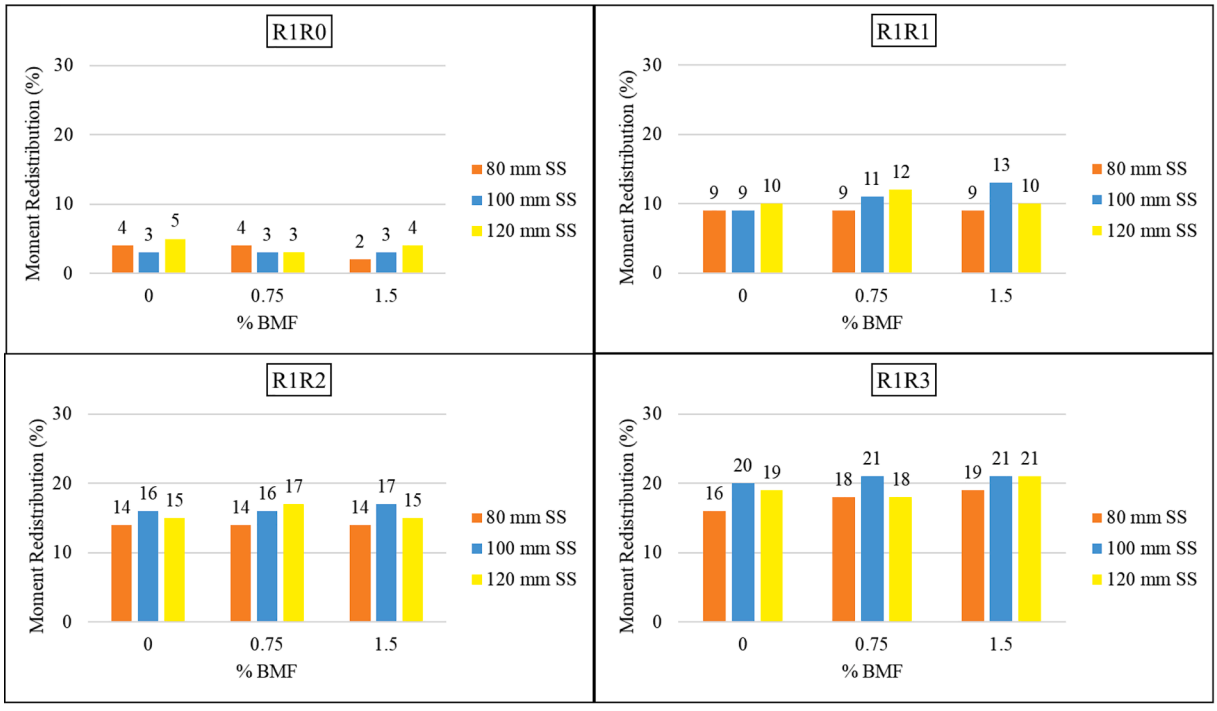

(b)

Fig. 4. Moment redistribution for different stirrups spacing and BMF percentages arranged as per the hogging reinforcement: (a) R0, (b) R1, (c) R2, and (d) R3.

trend between stirrups spacing and moment redistribution for all levels of reinforcement ratios and BMF, owing to the low influence of stirrups on the flexural behavior of the beams (Fig. 4(a)–(d)). This indicates that the moment redistribution of continuous beams is dominated by the longitudinal reinforcement configuration and the flexural capacity of sagging and hogging sections, as seen in Sections 3.1.1 and 3.1.2. This observation confirmes the results of El-Mogy et al. [38], who found that the moment redistribution of continuous beams is independent of the stirrups spacing.

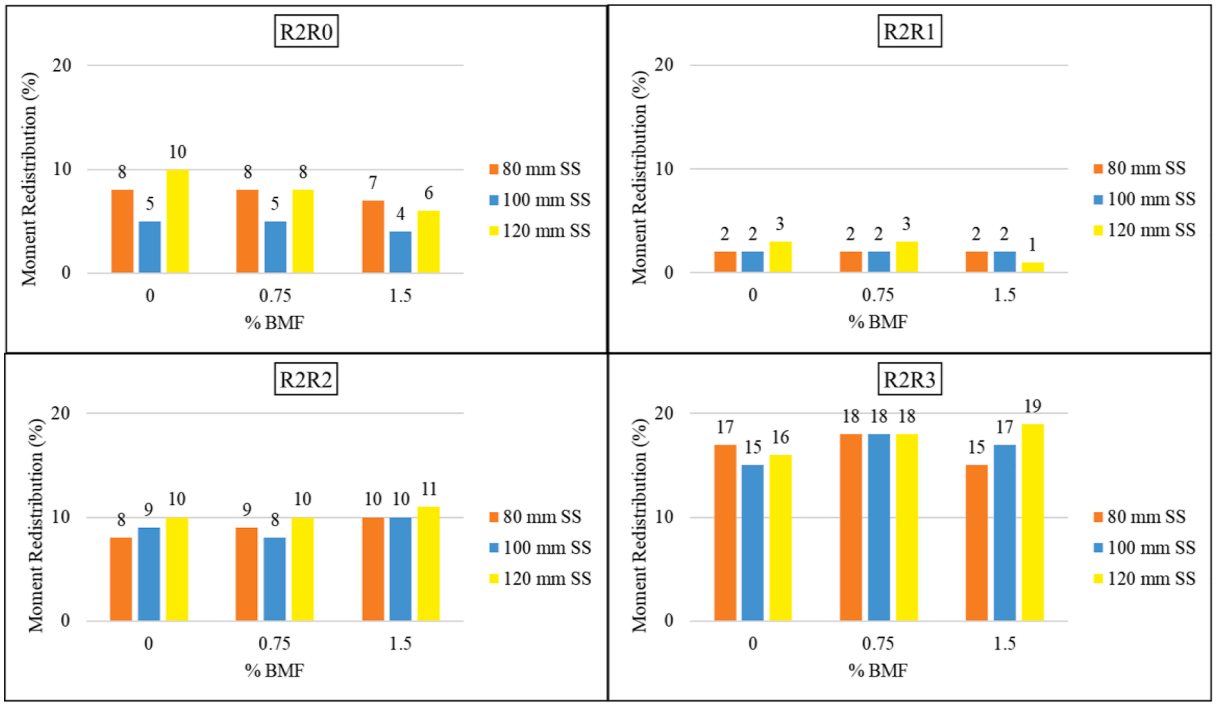

(c)

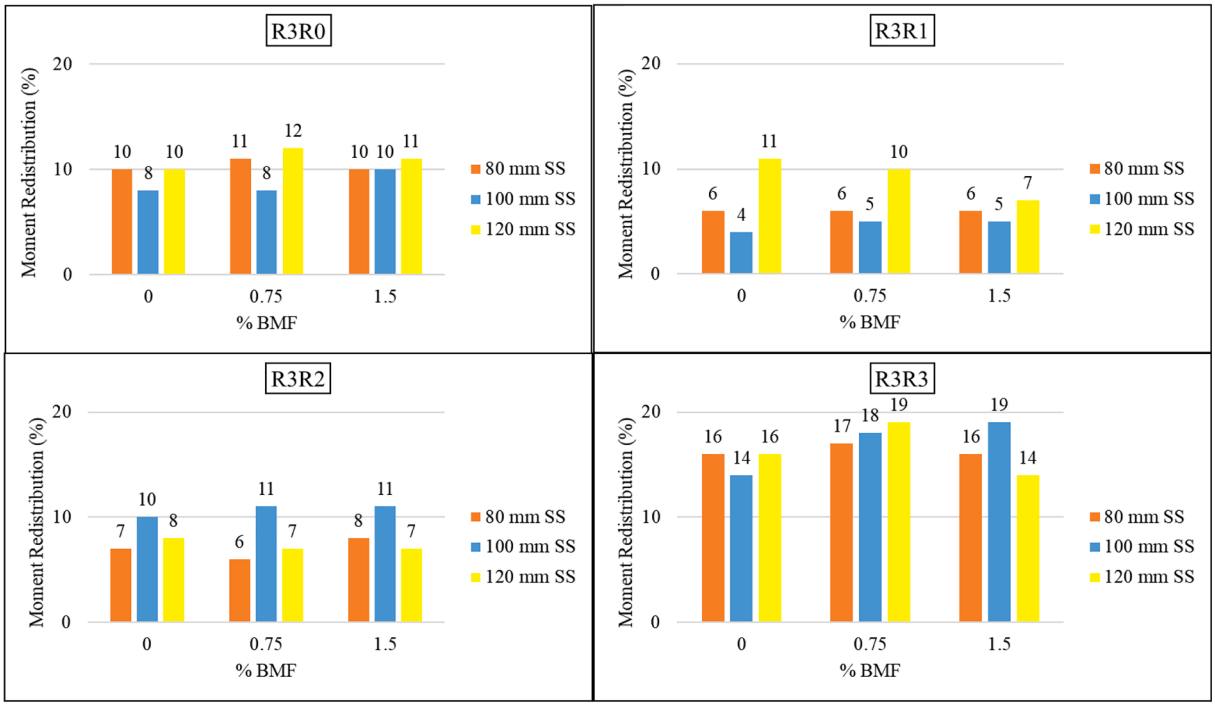

(d)

Fig. 4. (*continued*).

4. The statistical analysis

4.1. The correlation analysis

In this study, Pearson correlation test was performed to measure the degree of dependence between the test variables and moment redistribution. In general, correlation varies between −1 to +1; in which −1 indicates a perfect negative correlation and +1 indicates a perfect positive correlation. As could be noticed in Table 4, sagging reinforcement is the most influencing parameter on the beams' moment redistribution with a high positive correlation of 0.781. Furthermore, hogging reinforcement and beam moment redistribution were shown to have a modest negative correlation of 0.331, indicating that the moment redistribution is proportionally affected by the sagging-to-hogging reinforcement ratios. These results are in line with Akiel et al [19], El-Mogy et al. [29], and Abushanab et al. [47] experimental

Table 4
Pearson correlation between investigated variables and moment redistribution.

Variable	Moment redistribution
Sagging reinforcement	0.781
Hogging reinforcement	−0.331
BMF	0.029
Stirrups spacing	0.068

investigations. Moreover, in agreement with the parametric study results, both BMF and stirrups spacing showed negligible correlation with the moment redistribution.

4.2. The regression analysis

Regression analysis is a statistical tool commonly used to describe the relationship between dependent and independent variables. By developing such a relationship, a broader range of dependent variables could be estimated as an alternative tool to laboratory testing and FE simulations. Regression analysis is classified into two types: simple regression and multiple regression analysis. The simple regression is composed of a single independent variable, while the multiple regression is composed of more than one independent variable. A mathematical equation that represents the relationship between the dependent and independent variables is termed a regression model. The regression model is further classified into linear regression and non-linear regression models [56]. A general form of simple linear regression and multiple linear regression models are given in Eqs. (6) and (7), respectively:

$$Y = \beta_o + \beta_1 x_1 \tag{6}$$

$$Y = \beta_o + \beta_1 x_1 + \beta_2 x_2 + \cdots + \beta_n x_n \tag{7}$$

where Y is the dependent variable, β_o is the point where the line crosses the Y-axis (i.e., Y-intercept), β_1 is the slope of the line, $\beta_1, \beta_2, \cdots, \beta_n$ are the independent variable coefficients, and $x_1, x_2, \cdots, x_n$ are the independent variables. In the present work, a multiple linear regression analysis considering a confidence interval of 95% was carried out using the data presented in Section 3. The regression analysis aimed to statistically clarify the findings and establish a relationship between the moment redistribution of BFRP-BFRC continuous beams and reinforcement ratios, V_f of BMF, and stirrups spacing. The analysis was performed using Minitab 17 software [53], in which the moment redistribution was defined as the dependent variable, while reinforcement ratios, V_f of BMF, and stirrups spacing were defined as the independent variables. The regression coefficients were estimated using the curve fitting analysis. To improve the strength of the regression model, FE models R2R0, R3R0, and R3R1 were excluded from the regression analysis, as they experienced BFRP bar rupture failure mode and inverse moment redistribution. The proposed moment redistribution equation established from the regression analysis is shown in Eq. (8):

$$\mathrm{MR} = 3.72 + 0.041\mathrm{SR} - 0.025\mathrm{HR} + 0.44V_f + 0.021\mathrm{SS} \tag{8}$$

where MR is the moment redistribution (%), 3.72 is Y-intercept, SR is the sagging reinforcement area (mm^2), HR is the hogging reinforcement area (mm^2), V_f is the V_f of BMF (%), and SS is the stirrups spacing (mm). The proposed model had a coefficient of determination (R^2) of 87%, indicating an adequate fit model. Furthermore, the assumptions of the normal and random distribution, equal variance, and independence of the residuals were evaluated using the residual plots of the regression model, as shown in Fig. 5. The normal probability plot explains the distribution of the residual values. The residual distribution is considered normal when the points form a straight line and are close to the fitted line. The histogram plot assesses the normality of the residuals. The residual versus fit plot evaluates the random distribution and equal variance assumptions of the residuals. The residual versus order plot tests the independence of the residuals. From Fig. 5, it could be seen that most of the points in the probability plot are linearly distributed around the fitted line, except for two outliers at the ends. These outliers correspond to FE models R1R0 and R2R1, which have higher hogging reinforcement than sagging reinforcement. Moreover, the variability in the histogram plot is between −5 and 5 with no outliers in the developed model. Additionally, the residuals in the residual versus fit and residual

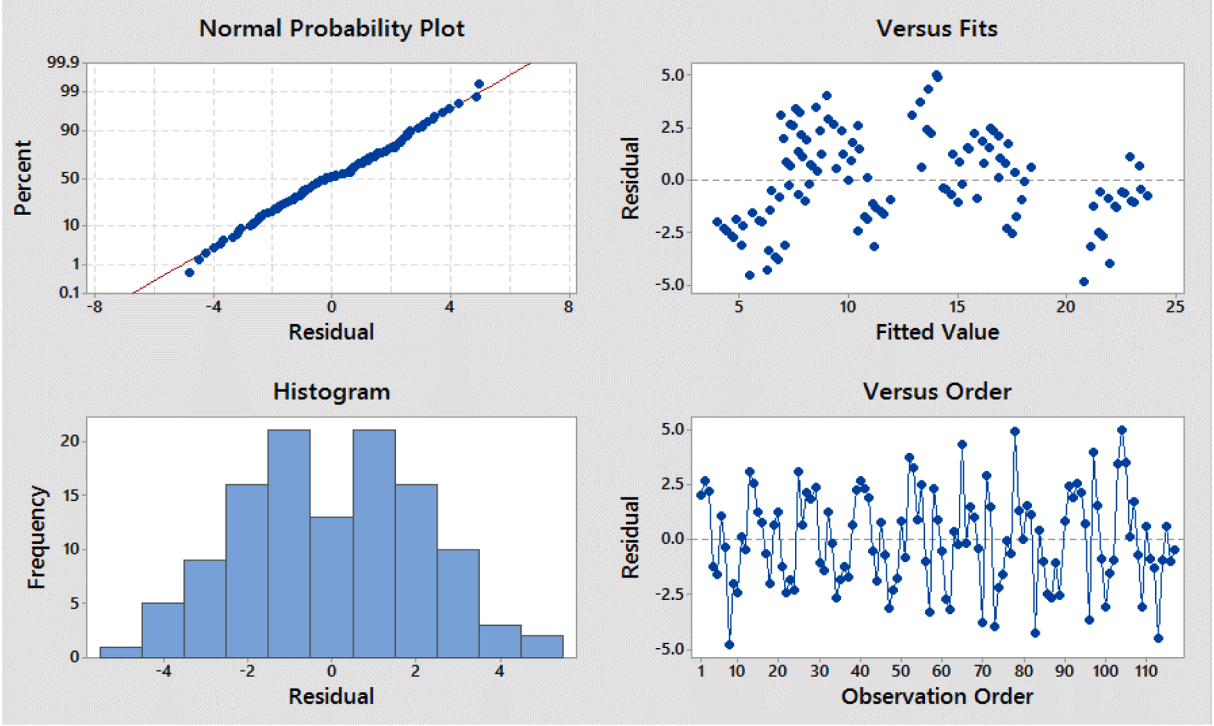

Fig. 5. Residual plots for the proposed regression model.

versus order plots are randomly distributed. This indicates that the residuals are independent of each other and have equal variance. Hence, the above-mentioned assumptions for the residuals are confirmed, and the data used is valid for the regression analysis. It is worth noting in Eq. (8) that the positive variable coefficients for the sagging reinforcement ratio, V_f of BMF, and stirrups spacing indicate that increasing these variables increases the moment redistribution, whereas the negative variable coefficient for the hogging reinforcement ratio indicates that the moment redistribution is inversely affected by the sagging reinforcement, which agrees with the results of the parametric study. Supporting Pearson correlation results, the effect of both BMF and stirrups spacing was negligible on the regression model. For example, a maximum increase in the beams' moment redistribution considering a V_f of BMF of 1.5% and stirrups spacing of 120 mm is 0.66% and 0.84%, respectively, as compared to beams with V_f of BMF of 0% and stirrups spacing of 80 mm. To this end, it can be concluded that the sagging-to-hogging reinforcement is the most influential parameter on the beams' moment redistribution.

4.3. Accuracy of the regression model

The accuracy of the proposed regression model was verified using the over-reinforced beam results reported by Abushanab et al. [47]. As shown in Table 5, the proposed regression model was capable of estimating the moment redistribution of the beams with experimental-to-estimated mean, standard deviation of the error, and coefficient of variance of 0.97, 0.09, and 9.08%, respectively. It should be noted that the estimated moment redistribution by Eq. (8) is a function of the geometry of the beams and properties of BFRP bars, BMF, and steel stirrups, and the results might vary if other beams' geometry or material properties are used. Therefore, further experimental work should be conducted to utilize the regression model for practical applications in order to obtain an accurate estimate of the moment redistribution of BFRP-BFRC continuous beams, as there is insufficient data in the literature.

5. Conclusions

A numerical one-factor-at-a-time parametric investigation was performed using 144 FE models to explore the influence of all possible combinations of reinforcement ratios, V_f of BMF, and stirrup spacings on the moment redistribution of BFRP-BFRC continuous beams. Afterward, a multiple linear regression using the parametric study data was conducted to establish a relationship between the investigated parameters and the moment redistribution of BFRP-BFRC continuous beams. The following conclusions are obtained from this parametric study:

1- The sagging reinforcement ratio had a more pronounced impact on the moment redistribution of BFRP-RC beams than the hogging reinforcement ratio. That was because the sagging reinforcement controls the beams' flexural strength.
2- A uniform moment redistribution occurred in FE models with hogging reinforcement ratios equal or lower than the sagging reinforcement ratio. The optimum sagging-to-hogging BFRP reinforcement ratio was found to be at least 1.6.
3- The BMF contribution in improving the beams' moment redistribution for FE models R1R3 with 120 mm stirrups spacing was 13% and 19% at $V_f = 0.75\%$ and 1.5%, respectively.
4- The parametric study showed no clear trend between the stirrups spacing and beams' moment redistribution. More experimental studies should be performed to confirm this conclusion.
5- The sagging-to-hogging reinforcement ratio was the most influential parameter on the beams' moment redistribution. This conclusion was observed by the parametric study and confirmed by the statistical analysis.

Table 5
Experimental to estimated moment redistribution ratios of BFRP-BFRC beams in Abushanab et al. [47].

FE model	V_f of BMF (%)	Stirrups spacing (mm)	$MR_{Exp.}$	$MR_{Est.}$	$\frac{MR_{Exp.}}{MR_{Est.}}$
R2R3	0	120	16.64	17.67	0.94
R2R3	0	80	17.62	16.83	1.05
R2R3	0.75	120	16.72	18.00	0.93
R3R2	0.75	120	8.30	7.62	1.09
R3R3	0.75	120	11.88	14.06	0.85
R2R3	1.50	120	17.40	18.33	0.95
Mean					0.97
SD					0.09
COV%					9.08

Note: MR = moment redistribution, Exp. = experimental, Est. = estimated, SD = standard deviation, and COV% = coefficient of variance.

6- The statistical analysis showed that BMF and stirrups spacing have negligible influence on the moment redistribution.
7- The developed regression model has accurately predicted the tested beams' moment redistribution with experimental-to-estimated mean, standard deviation of the error, and coefficient of variance of 0.97, 0.09, and 9.08%, respectively.

Finally, because there is very limited experimental data available in the literature to be compared with the proposed model, further research would be required to corroborate these findings and validate the developed model.

Declaration of Competing Interest

The authors declare that they have no known competing financial interests or personal relationships that could have appeared to influence the work reported in this paper.

Acknowledgment

This publication was made possible by GSRA grant GSRA6-1-0509-19022 from the Qatar National Research Fund (QNRF, a member of Qatar Foundation). The authors also show their gratitude to Qatar University for their financial support through internal research grants no. QUST-1-CENG-2020-17. Open Access funding provided by the Qatar National Library. The findings achieved herein are solely the responsibility of the authors.

Data availability

The raw/processed data required to reproduce these findings cannot be shared at this time as the data also forms part of an ongoing study.

References

[1] Sojobi AO, Liew KM. Flexural behaviour and efficiency of CFRP-laminate reinforced recycled concrete beams: Optimization using linear weighted sum method. Compos Struct 2021;260:113259. https://doi.org/10.1016/j.compstruct.2020.113259.
[2] Abed F, Alhafiz AR. Effect of basalt fibers on the flexural behavior of concrete beams reinforced with BFRP bars. Compos Struct 2019;215:23–34. https://doi.org/10.1016/j.compstruct.2019.02.050.
[3] Habeeb MN, Ashour AF. Flexural behavior of continuous GFRP reinforced concrete beams. J Compos Constr 2008;12(2):115–24. https://doi.org/10.1061/(ASCE)1090-0268(2008)12:2(115).
[4] Jiang F, Yang Q, Wang Y, Wang P, Hou D, Jin Z. Insights on the adhesive properties and debonding mechanism of CFRP/concrete interface under sulfate environment: From experiments to molecular dynamics. Constr Build Mater 2021;269:121247. https://doi.org/10.1016/j.conbuildmat.2020.121247.
[5] Cheon J, Lee M, Kim M. Study on the stab resistance mechanism and performance of the carbon, glass and aramid fiber reinforced polymer and hybrid composites. Compos Struct 2020;234:111690. https://doi.org/10.1016/j.compstruct.2019.111690.

[6] Attia K, El Refai A, Alnahhal W. Flexural behavior of basalt fiber-reinforced concrete slab strips with BFRP bars: Experimental testing and numerical simulation. J Compos Constr 2020;24(2):04020007. https://doi.org/10.1061/(ASCE)CC.1943-5614.0001002.
[7] Sim J, Park C, Moon DY. Characteristics of basalt fiber as a strengthening material for concrete structures. Compos Part B Eng 2005;36(6-7):504–12. https://doi.org/10.1016/j.compositesb:2005.02.002.
[8] Cai J, Pan J, Zhou X. Flexural behavior of basalt FRP reinforced ECC and concrete beams. Constr Build Mater 2017;142:423–30. https://doi.org/10.1016/j.conbuildmat.2017.03.087.
[9] El Refai A, Abed F. Concrete contribution to shear strength of beams reinforced with basalt fiber-reinforced bars. J Compos Constr 2016;20(4):04015082. https://doi.org/10.1061/(ASCE)CC.1943-5614.0000648.
[10] High C, Seliem HM, El-Safty A, Rizkalla SH. Use of basalt fibers for concrete structures. Constr Build Mater 2015;96:37–46. https://doi.org/10.1016/j.conbuildmat.2015.07.138.
[11] Elgabbas F, Ahmed EA, Asce M, Benmokrane B. Flexural Behavior of Concrete Beams Reinforced with Ribbed Basalt-FRP Bars under Static Loads 2017;21. https://doi.org/10.1061/(ASCE)CC.1943-5614.0000752.
[12] Atutis M, Valivonis J, Atutis E. Experimental study of concrete beams prestressed with basalt fiber reinforced polymers. Part I : Flexural behavior and serviceability. Compos Struct 2018;183:114–23. https://doi.org/10.1016/j.compstruct.2017.01.081.
[13] Tomlinson D, Fam A. Performance of concrete beams reinforced with basalt FRP for flexure and shear. J Compos Constr 2015;19(2):04014036. https://doi.org/10.1061/(ASCE)CC.1943-5614.0000491.
[14] Attia K, Alnahhal W, Elrefai A, Rihan Y. Flexural behavior of basalt fiber-reinforced concrete slab strips reinforced with BFRP and GFRP bars. Compos Struct 2019;211:1–12. https://doi.org/10.1016/j.compstruct.2018.12.016.
[15] Kara IF, Ashour AF. Flexural performance of FRP reinforced concrete beams. Compos Struct 2012;94(5):1616–25. https://doi.org/10.1016/j.compstruct.2011.12.012.
[16] Said M, Adam MA, Mahmoud AA, Shanour AS. Experimental and analytical shear evaluation of concrete beams reinforced with glass fiber reinforced polymers bars. Constr Build Mater 2016;102:574–91.
[17] Unsal I, Tokgoz S, Çağatay İ, Dundar C. A study on load-deflection behavior of two-span continuous concrete beams reinforced with GFRP and steel bars. Struct Eng Mech 2017;63:629–37. https://doi.org/10.12989/sem.2017.63.5.629.
[18] Rahman SMH, Mahmoud K, El-Salakawy E. Moment redistribution in glass fiber reinforced polymer-reinforced concrete continuous beams subjected to unsymmetrical loading. Eng Struct 2017;150:562–72. https://doi.org/10.1016/j.engstruct.2017.07.066.
[19] Akiel MS, El-Maaddawy T, El Refai A. Serviceability and moment redistribution of continuous concrete members reinforced with hybrid steel-BFRP bars. Constr Build Mater 2018;175:672–81. https://doi.org/10.1016/j.conbuildmat.2018.04.202.
[20] Mahroug MEM, Ashour AF, Lam D. Experimental response and code modelling of continuous concrete slabs reinforced with BFRP bars. Compos Struct 2014;107:664–74. https://doi.org/10.1016/j.compstruct.2013.08.029.
[21] Abushanab A, Alnahhal W. Performance of Basalt Fiber Reinforced Continuous Beams with Basalt FRP Bars. IOP Conf Ser Mater Sci Eng 2020;910:12004. https://doi.org/10.1088/1757-899x/910/1/012004.
[22] Grace NF, Soliman AK, Abdel-Sayed G, Saleh KR. Behavior and Ductility of Simple and Continuous FRP Reinforced Beams. J Compos Constr 1998;2(4):186–94. https://doi.org/10.1061/(ASCE)1090-0268(1998)2:4(186).
[23] Ashour AF, Habeeb MN. Continuous concrete beams reinforced with CFRP bars. Proc Inst Civ Eng Build - Proc Inst Civ Eng-Struct B 2008;161(6):349–57. https://doi.org/10.1680/stbu.2008.161.6.349.
[24] M.E.M. Mahroug A.F. Ashour D. Lam Tests of continuous concrete slabs reinforced with carbon fibre reinforced polymer bars Compos Part B Eng 66 2014 348 357 https://doi.org/https://doi.org/10.1016/j.compositesb.2014.06.003.
[25] Akiel M, El Maaddawy T, El Refai A. Flexural tests of continuous concrete slabs reinforced with basalt fiber-reinforced polymer bars, 2016.
[26] ACI (American Concrete Institute). “Building code requirements for structural concrete and commentary.” (ACI Comm 318-19) 2019.
[27] Canadian Standards Association. Design of concrete structures (CAN/CSA-A23.3-14). Toronto, Ontario, Canada: Canadian Standards Association; 2014.
[28] do Carmo RNF, Lopes SM. Required plastic rotation of RC beams. Proc Inst Civ Eng - Struct Build 2006;159(2):77–86. https://doi.org/10.1680/stbu.2006.159.2.77.
[29] El-Mogy M, El-Ragaby A, El-Salakawy E. Flexural behavior of continuous FRP-reinforced concrete beams. J Compos Constr 2010;14(6):669–80. https://doi.org/10.1061/(ASCE)CC.1943-5614.0000140.
[30] Piotr D, Krzysztof K. Research in redistribution of bending moments in the beams of reinforced concrete early loaded. Procedia Eng 2017;172:883–90. https://doi.org/10.1016/j.proeng.2017.02.096.
[31] Bagge N, O'Connor A, Elfgren L, Pedersen C. Moment redistribution in RC beams – A study of the influence of longitudinal and transverse reinforcement ratios and concrete strength. Eng Struct 2014;80:11–23. https://doi.org/10.1016/j.engstruct.2014.08.029.
[32] Kodur VKR, Campbell TI. Evaluation of Moment Redistribution in a Two-Span Continuous Prestressed Concrete Beam. ACI Struct J 1996;93. https://doi.org/10.14359/519.
[33] Ernst GC. Moment and shear redistribution in two-span continuous reinforced concrete beams. ACI J Proc 1958;55. https://doi.org/10.14359/11375.
[34] Rahman SMH, Mahmoud K, El-Salakawy E. Behavior of glass fiber-reinforced polymer reinforced concrete continuous T-beams. J Compos Constr 2017;21(2):04016085. https://doi.org/10.1061/(ASCE)CC.1943-5614.0000740.
[35] Gravina RJ, Smith ST. Flexural behaviour of indeterminate concrete beams reinforced with FRP bars. Eng Struct 2008;30(9):2370–80. https://doi.org/10.1016/j.engstruct.2007.12.019.
[36] Razaqpur AG, Mostofinejad D. Experimental Study of Shear Behavior of Continuous Beams Reinforced with Carbon Fiber Reinforced Polymer. In: Dolan CW, Rizkalla SH, Nanni A, editors. 4th Int. Symp., Fiber Reinf. Polym. Reinf. Reinf. Concr. Struct., vol. 188, 1999, p. 169–78.
[37] Kara IF, Köroğlu MA, Ashour AF. Tests of continuous concrete slabs reinforced with basalt fibre reinforced plastic bars 2017. https://doi.org/10.14359/51689784.
[38] El-Mogy M, El-Ragaby A, El-Salakawy E. Effect of transverse reinforcement on the flexural behavior of continuous concrete beams reinforced with FRP. J Compos Constr 2011;15(5):672–81. https://doi.org/10.1061/(ASCE)CC.1943-5614.0000215.
[39] ACI (American Concrete Institute Committee 440). Guide for the Design and Construction of Structural Concrete Reinforced with Fibre-Reinforced Polymer (FRP) Bars. (ACI 4401R-15) 2015. https://doi.org/10.1061/40753(171)158.
[40] JSCE(Japan Society of Civil Engineers). Recommendation for design and construction of concrete structures using continuous fiber reinforcing materials. 1997:1–58.
[41] CSA (Canadian Standards Association). Design and construction of building components with fiber reinforced polymers. (CSA-S806-12) 2012.
[42] ISIS (Intelligent Sensing for Innovative Structures). Reinforcing Concrete Structures with Fibre Reinforced Polymers. 2007.
[43] Wang H, Belarbi A. Ductility characteristics of fiber-reinforced-concrete beams reinforced with FRP rebars. Constr Build Mater 2011;25(5):2391–401. https://doi.org/10.1016/j.conbuildmat.2010.11.040.
[44] Yang J-M, Min K-H, Shin H-O, Yoon Y-S. Effect of steel and synthetic fibers on flexural behavior of high-strength concrete beams reinforced with FRP bars. Compos Part B Eng 2012;43(3):1077–86. https://doi.org/10.1016/j.compositesb:2012.01.044.
[45] Issa MS, Metwally IM, Elzeiny SM. Influence of fibers on flexural behavior and ductility of concrete beams reinforced with GFRP rebars. Eng Struct 2011;33(5):1754–63. https://doi.org/10.1016/j.engstruct.2011.02.014.
[46] Visintin P, Mohamad Ali MS, Xie T, Sturm AB. Experimental investigation of moment redistribution in ultra-high performance fibre reinforced concrete beams. Constr Build Mater 2018;166:433–44. https://doi.org/10.1016/j.conbuildmat.2018.01.156.
[47] Abushanab A, Alnahhal W, Farraj M. Structural performance and moment redistribution of basalt FRC continuous beams reinforced with basalt FRP bars. Eng Struct 2021;240:112390. https://doi.org/10.1016/j.engstruct.2021.112390.
[48] Shafiq N, Ayub T, Khan SU. Investigating the performance of PVA and basalt fibre reinforced beams subjected to flexural action. Compos Struct 2016;153:30–41. https://doi.org/10.1016/j.compstruct.2016.06.008.
[49] Al-Hamrani A, Alnahhal W. Shear behavior of basalt FRC beams reinforced with basalt FRP bars and glass FRP stirrups: Experimental and analytical investigations. Eng Struct 2021;242:112612. https://doi.org/10.1016/j.engstruct.2021.112612.
[50] Abushanab AH. Parametric study on moment redistribution of fiber reinforced concrete continuous beams with basalt FRP bars. Qatar University, 2019. https://doi.org/hdl.handle.net/10576/12331.
[51] Abaqus 6.14 Documentation 2014.
[52] Ayub T, Khan SU, Shafiq N. Flexural modelling and finite element analysis of FRC beams reinforced with PVA and basalt fibres and their validation. Adv Civ Eng 2018;2018:1–18. https://doi.org/10.1155/2018/8060852.
[53] Minitab I. MINITAB release 17: statistical software for windows. USA: Minitab Inc; 2014. p. 371.
[54] Santos P, Laranja G, França PM, Correia JR. Ductility and moment redistribution capacity of multi-span T-section concrete beams reinforced with GFRP bars. Constr Build Mater 2013;49:949–61. https://doi.org/10.1016/j.conbuildmat.2013.01.014.
[55] Alnahhal W, Aljidda O. Flexural behavior of basalt fiber reinforced concrete beams with recycled concrete coarse aggregates. Constr Build Mater 2018;169:165–78. https://doi.org/10.1016/j.conbuildmat.2018.02.135.
[56] Tripepi G, Jager KJ, Dekker FW, Zoccali C. Linear and logistic regression analysis. Kidney Int 2008;73(7):806–10. https://doi.org/10.1038/sj.ki.5002787.